Journal of Magnetics 5(3), 81-84 (2000)

Measurements of Local Coercivity Distribution in Ferromagnetic Films Using Magneto-Optical Microscope Magnetometer (MOMM)

Sug-Bong Choe and Sung-Chul Shin

Department of Physics and Center for Nanospinics of Spintronic Materials, Korea Advanced Institute of Science and Technology, Taejon 305-701, Korea

(Received 16 June 2000)

A magneto-optical microscope magnetometer (MOMM) has been developed to simultaneously measure 2-dimensional array hysteresis loops of each local area of 320×320-nm^2 spots on ferromagnetic films, in addition to grabbing time-resolved domain evolution patterns. Using the system, spatial distribution of local coercivity can be quantitatively generated and then, compared directly with domain patterns grabbed at precisely the same position of a sample. It is clearly demonstrated that local coercivity distribution governs domain reversal behavior via a thermally activated relaxation process.

1. Introduction

Hysteresis in magnetic materials motivates fascinating interests in magnetism and also, it provides versatile tools for characterization of magnetic properties [1]. Recently, interest in magnetism is rapidly grown in exploration of the microscopic properties of magnetic materials having the physical and/or chemical microstructures, motivated by achieving high performance in magnetic application as well as solving fundamental curiosity in magnetism [2-5]. Quantitative determination of hysteresis and characterization of magnetic properties near a nanometer-scale spatial resolution are essential in understanding of their dependences on the microstructures at appropriate length scale as well as in search for new exotic magnetic materials.

Most hysteresis characterization techniques including VSM [6], AGM [7], MOKE magnetometer [8], and SQUID magnetometer [9] basically measure the magnetic properties of a whole sample and therefore, they can not provide micromagnetic properties of the local areas of the sample. On the other hand, many magnetic imaging techniques including MFM [10], SEMPA [11], SPLEEM [12], TEM [13], and STM [14] have been devoted to investigate microscopic domain structures with spatial resolution of some tens of nm. However, despite the high spatial resolution of these techniques, it is hard to draw any quantitative magnetic information due to the limitations imposed by applying a magnetic field and/or slow data acquisition times.

The present study was motivated to characterize the local magnetic properties by measuring spatially-resolved hysteresis loops of each local area. For this study, we have developed a magneto-optical microscope magnetometer (MOMM) capable of simultaneous measurements of 8,000 local hysteresis loops corresponding to each 320×320-nm^2 area spots on a ferromagnetic film. Using this system, we can generate spatial distribution maps of local magnetic properties including coercivity, remnant, and so on, determined from each local hysteresis loop. Note that the local magnetic properties can be directly analyzed with the domain evolution patterns grabbed at *precisely the same* position of a sample, since the system also provides the time-resolved domain pattern grabbing in real time [15]. This Letter demonstrates the direct correlation between the local coercivity distribution and the domain reversal dynamics.

The MOMM system mainly consists of an optical polarizing microscope capable of $\times 1{,}000$ magnification with spatial resolution of 300 nm and Kerr-angle resolution of 0.2 degree [15]. To measure hysteresis loops, the system is equipped with a computer-controlled electromagnet to sweep the external field in the range of ± 5 kOe. Domain images are captured by a CCD camera system interfaced to the computer. The images are composed of the light intensity distribution measured by the CCD array of 100×80 pixels, where a unit pixel corresponds to the local area of 320×320 nm^2 of the film surface. By storing the domain images while sweeping the external magnetic field H, it is possible to obtain an array of the local intensity variation $I_{xy}(H)$ as a function of H. This is done by simultaneously tracing the intensity variation at every corresponding $(x,y)th$ CCD pixels. Figure 1(a) shows a typical dependence of the intensity variation on an applied magnetic field H. The intensity $I_{xy}(H)$ is related with the Kerr rotation angle $q_{xy}(H)$ by

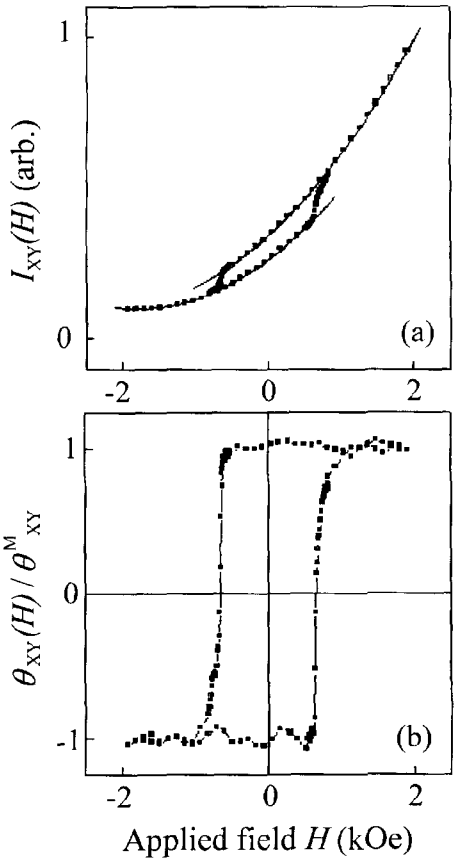

Fig. 1. (a) Typical local-intensity variation $I_{xy}(H)$ measured by the $(x,y)th$ CCD pixel. The solid lines are the fitting curves given by Eq. (1) for the two saturated states. (b) The normalized Kerr hysteresis loop $\theta_{xy}(H)$ of the local sample area of 320×320 nm^2 generated from the intensity variation shown in (a).

$$I_{xy}(H)=I_{xy}^{0}+C_{xy}\sin^2(\theta_{xy}(H)+\alpha_{xy}H+\Delta\theta_{xy}), \quad (1)$$

where I_{xy}^{0} is the intensity offset of the corresponding CCD pixel, C_{xy} is the proportionality coefficient between the intensity and the Kerr rotation angle, α_{xy} is the Faraday coefficient at the objective lens of the microscope, and $\Delta\theta_{xy}$ is the angle between the polarizer and analyzer [16]. By fitting the measured $I_{xy}(H)$ versus H in Eq. (1) for the two saturated states of $q_{xy}(H) = \pm q_{xy}^{M}$ as shown by the solid lines in Figure 1(a), one can determine the values of I_{xy}^{0}, $C_{xy}\alpha_{xy}^{2}$, $\Delta\theta_{xy}/\alpha_{xy}$, and $\theta_{xy}^{M}/\alpha_{xy}$ under the approximation of $\sin\theta \sim \theta$ for a small θ. Then, the normalized Kerr hysteresis loop can be generated from the intensity variation with the fitting quantities by

$$\frac{\theta_{xy}(H)}{\theta_{xy}^{M}} = \frac{\alpha_{xy}}{\theta_{xy}^{M}} \cdot \left(\sqrt{\frac{I_{xy}(H)-I_{xy}^{0}}{C_{xy}\alpha_{xy}^{2}}} - H \right) - \frac{\Delta\theta_{xy}}{\theta_{xy}^{M}} \quad (2)$$

Figure 1(b) shows the normalized Kerr hysteresis loop generated from the intensity variation shown in Figure 1(a). It should be emphasized that the Kerr hysteresis loop is obtained for every CCD pixel and thus, one can generate the maps of the local magnetic properties measured from the corresponding hysteresis loop of each CCD pixel.

The present system has been applied to characterize the local magnetic properties of Co/Pd multilayered system, which has been intensively investigated as one of the prospective candidates for the high-density magneto-optical recording media [15-19]. The multilayer structure was achieved by alternatively exposing the glass substrate to two e-beam sources of Co and Pd under a base pressure of 2.0×10^{-7} Torr at ambient temperature. The layer thickness was controlled within 4% accuracy [15]. Low-angle x-ray diffraction studies using Cu $K\alpha$ radiation revealed that all samples had distinct peaks indicating an existence of the multilayer structure. High-angle x-ray diffraction studies showed that the samples grew along the <111> cubic orientation. All the samples have perpendicular magnetic anisotropy and show hysteresis loops of unit squareness. We will designate the samples as $(t_{Co}$-Å Co/t_{Pd}-Å Pd$)_n$, where t_{Co} is the Co-sublayer thickness, t_{Pd} is the Pd-sublayer thickness, and n is the number of repeats.

The spatial distribution maps of the local coercivity have been generated from the 2-dimensional array of the Kerr hysteresis loops measured at each local area of 320×320 nm^2 on the Co/Pd multilayered sample surface. The hysteresis loops were obtained by measuring the Kerr intensity with every 10-Oe interval and the field sweep rate of 25 Oe/s. The Kerr intensity was averaged by 16-times measurements of major loops for a given sample, since the reversal phenomenon is inherently governed by statistical reversal probability. Care was taken to maintain the observation sight of the MOMM measurement preventing the thermal and/or gravitational drift and the mechanical vibration of the sample stage during the measurement. The coercivity H_C was determined by interpolating the applied field for the condition of θ_{xy} $(H_C) = 0$. The experimental error in coercivity determination was confirmed to be smaller than 2 Oe for these particular Co/Pd multilayers having the maximum Kerr rotational angle of about 0.15 degree.

Interestingly, the coercivity of the Co/Pd multilayers was found to be spatially nonuniform on submicrometer scale on the sample. Figure 2 demonstrates the local coercivity distribution $H_C(x,y)$ of the (2.5-Å Co/11-Å Pd)$_{10}$ sample in gray level onto the 2-dimensional XY plane, where each map corresponds to a sample surface area of 32.0×25.6 mm^2. The figure vividly shows the spatial fluctuation of the local coercivity on submicrometer scale. The difference in the loop shape and the coercivity is clearly seen between the plots in the left and right side of the figures, which show the hysteresis loops measured at the unit pixels corresponding to two different local spots designated by each arrow. The standard deviation of the local coercivity distribution for this sample was determined to be 19 Oe. The fluctuation of the local coercivity is possibly ascribed to the structural irregularity due to the possible accumulation of the lattice misfits, residual stress, and other defects, especially at the

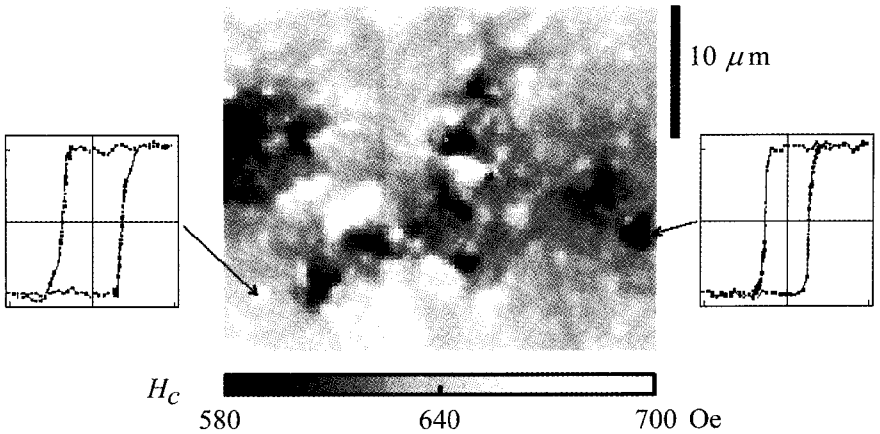

Fig. 2. The local coercivity distributions $H_C(x,y)$ of the (2.5-Å Co/11-Å Pd)$_{10}$ sample. The plots show the hysteresis loops measured at the unit pixels corresponding to two local areas designated by each arrow. Here, x-axis is an applied field ranging from -2 kOe to 2 kOe and y-axis is the normalized Kerr rotational angle.

interfaces during deposition process in high vacuum, since the coercivity is a structure-sensitive magnetic property [20]. Therefore, one might expect a larger variation in the local coercivity with increasing the number of repeats; it was indeed observed in our Co/Pd multilayer samples [16].

To examine the influence of the spatial fluctuation of the local coercivity on the magnetization process, we have investigated the magnetization reversal dynamics of the Co/Pd multilayers at *precisely the same* position of the sample via the time-resolved observation of domain evolution by applying a reverse magnetic field starting from the saturated state [15]. Figure 3(a) shows the domain evolution patterns for the (2.5 Å Co/11-Å Pd)$_{10}$ sample, where the gray level in the figure designates the time $\tau(x,y)$ required for the corresponding region of the $(x,y)th$ pixel to reverse. Most interestingly, one can notice that the reversal pattern in Figure 3(a) is truly coincident with the local coercivity distribution in Figure 1. This directly demonstrates the close correlation between the local coercivity distribution and domain reversal pattern on the submicron scale.

For a quantitative analysis of the correlation, we have measured the number of pixels $N(H_C, \tau)$ by counting the pixels having the values of the local coercivity $H_C(x,y)$ and the local reversal time $\tau(x,y)$ at the same $(x,y)th$ pixel in the corresponding map. Figure 3(b) illustrates the correlated distribution of the number of pixels $N(H_C,\tau)$ in logarithmic scale in H_C-τ coordinates. In the figure, it is very clearly seen that the local reversal time is truly correlated with the local coercivity, which implies that the local domain dynamics during magnetization reversal is directly governed by the local coercivity.

The reversal mechanism taking into account the local coercivity distribution could be analyzed within the context of a thermally activated relaxation process. The half reversal time τ, the time needed to reverse half the volume of the sample, is known to be exponentially dependent on an applied field H [21]. By considering the local coercivity distribution $H_C(x,y)$, the half reversal time $\tau(x,y)$ of the mag-

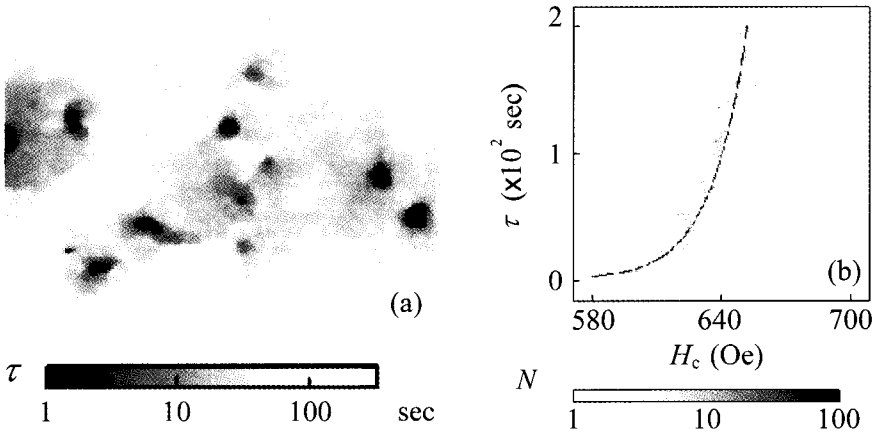

Fig. 3. (a) The time-resolved domain reversal pattern of the (2.5-Å Co/11-Å Pd)$_{10}$ sample at exactly the same position shown in Figure refcoercivity. The gray level corresponds to the time $\tau(x,y)$ in a logarithmic scale for reversal of the corresponding region (x,y). (b) The correlated distribution of the number of pixels $N(H_C,\tau)$ with logarithmic gray level in H_C-τ coordinate for the (2.5-Å Co/11-Å Pd)$_{10}$ sample. The solid line represents the best fit using Eq. (3).

netization M_S of a volume V_A located at (x,y) is given by

$$\tau(x, y)=\tau_0 \exp\left(\frac{V_A M_S}{k_B T}(H_C(x, y)-H)\right), \quad (3)$$

where t_0 is the characteristic reversal time for $H = H_C(x,y)$, k_B is Boltzmann's constant, and T is temperature [21]. It is clearly demonstrated that the correlated distribution can be quantitatively characterized by Eq. (3) as shown by the solid line in Figure 3(b). The activation volume V_A of the sample is determined to 7.9×10^{-18} cm^3, which is almost identical to the previous value determined via the field dependence of the half reversal time in the whole area of the sample [22].

In conclusion, we have developed a magneto-optical microscope magnetometer (MOMM) capable of simultaneous measurements of local hysteresis loops with the 320-nm spatial resolution. Using the MOMM system, local coercivity distribution can be generated from a 2-dimensional array of hysteresis loops at each pixel of 320×320 nm^2. The local coercivity distribution of Co/Pd multilayered samples has been investigated and interestingly, the coercivity of the samples was found to be spatially nonuniform on submicrometer scale. The local coercivity distribution is directly analyzed with the domain reversal patterns grabbed at *precisely the same* position, and it is clearly demonstrated that the local coercivity distribution governs the domain reversal dynamics via a thermally activated relaxation process.

Acknowledgements

This work was supported by the Creative Research Initiatives of the Ministry of Science and Technology of Korea.

References

[1] G. Bertotti, *Hysteresis in Magnetism*, Academic Press, San Diego (1998), Part IV.
[2] S.-C. Shin, Appl. Surf. Sci., **65**, 110 (1993).
[3] S. Gider, B.-U. Runge, A. C. Marley, and S. S. P. Parkin, Science, **281**, 797 (1998).
[4] T. Aign, P. Meyer, S. Lemerle, J. P. Jamet, J. Ferré, V. Mathet, C. Chappert, J. Gierak, C. Vieu, F. Rousseaux, H. Launios, and H. Bernas, Phys. Rev. Lett., **81**, 5656 (1998).
[5] M. Hehn, K. Ounadjela, J.-P. Bucher, F. Rousseaux, D. Decanini, B. Bartenlian, and C. Chappert, Science, **272**, 1782 (1996).
[6] S. Foner, IEEE Trans. Magn., **17**, 3358 (1981).
[7] G. A. Gibson and S. Schultz, J. Appl. Phys., **69**, 5880 (1991).
[8] K. Sato, H. Hongu, H. Ikekame, and Y. Tosaka, Jpn. J. Appl. Phys., **32**, 989 (1993).
[9] W. Webb, IEEE Trans. Magn., **8**, 51 (1972).
[10] E. Dan Dahlberg and J.-G. Zhu, Phys. Today, **48**, 34 (1995).
[11] M. R. Scheinfein, J. Unguris, M. H. Kelley, D. T. Pierce, and R. J. Celotta, Rev. Sci. Instrum, **61**, 2501 (1990).
[12] E. Bauer, Rep. Prog. Phys., **57**, 895 (1994).
[13] E. Betzig, J. K. Trauman, R. Wolfe, E. M. Gyorgy, P. L. FInn, M. H. Kryder and C.-H. Chang, Appl. Phys. Lett., **61**, 142 (1992).
[14] R. Wiesendanger, H.-J. Guntherodt, G. Guntherodt, R. J. Gambino, and R. Ruf, Phys. Rev. Lett., **65**, 247 (1990).
[15] S.-B. Choe and S.-C. Shin, Phys. Rev., B **57**, 1085 (1998); Appl. Phys. Lett., **70**, 3612 (1997).
[16] S.-B. Choe and S.-C. Shin, J. Appl. Phys., **87**, 6848 (2000).
[17] P. F. Carcia, A. D. Meinhaldt, and A. Suna, Appl. Phys. Lett., **47**, 178 (1985).
[18] S.-C. Shin, J.-H. Kim, and D.-H. Ahn, J. Appl. Phys., **69**, 5664 (1991).
[19] D. G. Stinston and S.-C. Shin, J. Appl. Phys., **67**, 4459 (1990).
[20] H. Kronmuller, Phys. Stat. Sol., (b) **144**, 385 (1987).
[21] J. Pommier, P. Meyer, G. Pónissard, J. Ferré, P. Bruno, and D. Renard, Phys. Rev. Lett., **65**, 2054 (1990).
[22] S.-B. Choe and S.-C. Shin, J. Appl. Phys., **87**, 5076 (2000).